https://doi.org/10.5194/tc-2022-206
Preprint. Discussion started: 1 November 2022

The Cryosphere Discussions

Direct measurement of warm Atlantic Intermediate Water close to the grounding line of Nioghalvfjerdsfjorden (79N) Glacier, North-east Greenland.

Michael J. Bentley[1], James A. Smith[2], Stewart S.R. Jamieson[1], Margaret R. Lindeman[3], Brice R. Rea[4], Angelika Humbert[5,6], Timothy P. Lane[7], Christopher M. Darvill[8], Jeremy M. Lloyd[1], Fiamma Straneo[3], Veit Helm[5], and David H. Roberts[1].

[1]*Department of Geography, South Rd, Durham University, Durham, DH1 3LE, UK.*

[2]*British Antarctic Survey, High Cross, Madingley Rd, Cambridge, CB3 0ET, UK*

[3]*Scripps Institution of Oceanography, University of California, San Diego, CA, USA*

[4]*Geography and Environment, School of Geosciences, University of Aberdeen, Elphinstone Road, Aberdeen, AB24 3UF, UK*

[5]*Alfred-Wegener-Institut, Helmholtz Zentrum für Polar- und Meeresforschung, Bremerhaven, Germany*

[6]*Faculty of Geosciences, University of Bremen, Bremen, Germany*

[7]*School of Biological and Environmental Sciences, Liverpool John Moores University, Liverpool, L3 3AF, UK*

[8]*Department of Geography, The University of Manchester, Oxford Road, Manchester, M13 9PL, UK*

Correspondence to: Michael J. Bentley (m.j.bentley@durham.ac.uk)

Abstract. The North-East Greenland Ice Stream has recently seen significant change to its floating margins, and has been identified as vulnerable to future climate warming. Inflow of warm Atlantic Intermediate Water (AIW) from the continental shelf has been observed in the vicinity of the Nioghalvfjerdsfjorden (79N) Glacier calving front, but AIW penetration deep into the ice shelf cavity has not been observed directly. Here, we report temperature and salinity measurements from profiles in an epishelf lake, which provide the first direct evidence of AIW proximal to the grounding line of 79N Glacier, over 50 km from the calving front. We also report evidence for partial un-grounding of the margin of 79N taking place at the western end of the epishelf lake. Comparison of our measurements to those close to the calving front shows that AIW transits the cavity to reach the grounding line within a few months. The observations provide support for modelling studies that infer AIW-driven basal melt proximal to the grounding line and demonstrate that offshore oceanographic changes can be rapidly transmitted throughout the sub-ice shelf cavity, with implications for near-future stability of the ice stream.

1 Background and rationale

The North-East Greenland Ice Stream (NEGIS) is the largest ice stream in Greenland and the main artery for ice discharge from the NE sector of the ice sheet to the North Atlantic, draining an area of 200,000 km^2 or 12% of the ice sheet (Mouginot et al., 2015). Unlike many other sectors of the Greenland Ice Sheet, NEGIS and the ice shelves that front it exhibited little response to atmospheric and oceanic warming for the decades immediately prior to the mid-2000s. However, recent ice shelf loss and rapid grounding-line retreat post-2010 suggest that this sector of the Greenland Ice Sheet, and NEGIS, are starting to respond to atmospheric/ocean change (Khan et al., 2014; Mouginot et al., 2015; Mayer et al., 2018; Lindeman et al., 2020; An et al., 2021). Model projections suggest that ocean warming around Greenland will double by 2100 (Yin et al., 2011) and air temperature is likely to increase significantly in northeast Greenland (AMAP, 2011; Hanna et al., 2020). This means that the future evolution of the NEGIS catchment

https://doi.org/10.5194/tc-2022-206
Preprint. Discussion started: 1 November 2022


The Cryosphere Discussions
Open Access
EGU

is important, not only for understanding changing dynamics in this sector of the ice sheet but also for predicting future sea level rise as the catchment holds a volume of ice equivalent to 1.1 m of sea level rise (Mouginot et al., 2015; An et al., 2021).

The streaming onset zone of NEGIS is at the central ice divide of the ice sheet, and the ice stream branches into three outlet glaciers (Nioghalvfjerdsfjorden Glacier ('79N Glacier'), Zachariae Isstrøm (ZI) and Storstrømmen Glacier (SG); Figure 1) as it approaches the ice sheet margin. NEGIS flows at ~1200 m a^{-1} and upstream from the 79N Glacier grounding line (~600 m below sea-level) the basin floor deepens to ~1000 mbsl (Bamber et al., 2013). 79N Glacier is fronted by an ice shelf ~80 km long (Fig. 1) which is 100 to 300 m thick east of the grounding line, with fjord depths in the cavity reaching >900 mbsl (Mayer et al., 2000; Morlighem et al., 2017). Khan et al. (2014) report 25 years of relative stability of both 79N Glacier and ZI prior to the mid-2000s after which there have been sporadic periods of dynamic thinning and flow acceleration. The ZI ice shelf in particular has undergone rapid retreat (~40 km), and post 2010 it disintegrated completely leaving a grounded tidewater margin which is now retreating along a retrograde slope. Khan et al. (2014) link these changes to increased air temperatures and sea ice loss, with several studies also implicating ocean warming (Mouginot et al., 2015; An et al., 2021) which may have significantly increased submarine melt rates of the ice shelves and the grounded tidewater margins. Humbert et al (submitted) also identify a recent shift in calving style and fracturing at the calving front of 79N Glacier.

A number of studies have highlighted the likely influence of incursions of warm Atlantic Intermediate Water (AIW) on 79N Glacier and the fronting ice shelf. Based on the rapid decrease in thickness of the ice shelf, to only 330 m within 5 km of the 79N Glacier grounding line, Mayer et al. (2000) estimated very high basal melt rates of 40 ma^{-1} close to the grounding line and suggested these may be due to the presence of AIW. Schaffer et al. (2017) showed that AIW crosses the continental shelf, at depths >150-200 m, via Norske Trough and along a continuous deep channel (> 370 mbsl) that extends to the main (southern) calving front (Schaeffer et al., 2017), allowing AIW to potentially reach the grounding line of 79N Glacier. The exchange flow across the 79N fjord front is primarily controlled by variability in AIW layer thickness, circulation on the continental shelf and bathymetry (Schaffer et al., 2020; von Albedyll et al., 2021). Three gateways have been identified at the main calving front where AIW enters or leaves the sub-ice shelf cavity (Fig. 1a) (Schaffer et al., 2020; von Albedyll et al., 2021). A sill blocks other parts of the southern entrance (Schaffer et al., 2020; von Albedyll et al., 2021) and AIW is unable to enter at the northern calving front in Dijmphna Sund because of a shallow (170 m) sill that acts to block the deeper inflow (Wilson and Straneo, 2015). There is only one measurement of AIW in the cavity, where it has been detected in a rift in the 79N ice tongue, located ~10 km behind the calving front (Wilson and Straneo, 2015; Lindeman et al., 2020). A record from an Ice Tethered Mooring (ITM) situated in this rift reveals that AIW is present in the cavity year-round, with maximum temperatures reaching ~1.5°C at 500 m depth in July 2017 (Lindeman et al., 2020). Details of the circulation of AIW in the cavity remain speculative, as incursion of the AIW into the cavity has not been demonstrated beyond the rift site. Von Albedyll et al. (2021) suggested that a Coriolis-driven circulation would result in the deflection of the main outflow to the southernmost part of the cavity. However, data from moorings actually show that while there is some outflow through two of the exits along the southern front, the strongest outflow takes place through Dijmphna Sund, across the northern calving front (Lindeman et al., 2020; von Albedyll et al., 2021). The implication is that the sub-ice shelf morphology and/or fjord bathymetry are steering the water circulation within the cavity (von Albedyll et al., 2021).

AIW has warmed in recent years in the Fram Strait (Beszczynska-Moller et al., 2012), in the Arctic Ocean (Polyakov et al., 2012) and in the Norske Trough system (Schaffer et al., 2017). In the latter case a warming of 0.5 °C was seen

https://doi.org/10.5194/tc-2022-206
Preprint. Discussion started: 1 November 2022

between 1979-1999 and 2000-2016. This appears to be reflected within the 79N fjord with CTD profiles showing an increasingly warmer, shallower, high salinity, AIW layer beneath the ice shelf since 1996 (Mayer et al., 2018; Lindeman et al., 2020). For example, Mayer et al. (2018) indicate an increase of 0.5°C at 175 m depth, which would equate to a potential increase in melt rate of ~5 ma^{-1}, following Rignot and Jacobs (2002) who suggested that an increase of 0.1 °C in sub-ice shelf water temperature corresponds to a change in basal melt of ice shelves of ~1 m a^{-1}.

Mayer et al. (2018) used satellite imagery to track the migration of a compressional ridge (which they referred to as 'Midgardsormen ridge'), formed on the ice shelf surface as it flows obliquely across a grounding line (from floating to grounded) along the northern side of the fjord (Fig. 1a). Thinning of the ice shelf since at least 1998, at a rate of up to 12 m a^{-1}, resulted in landward migration of the grounding line/Midgardsormen. Mass balance calculations and flow modelling suggest that glacier dynamics or atmospheric warming alone are unable to explain the magnitude of this thinning trend. However, a simple plume model for the ice shelf cavity showed that penetration of warm water to the grounding line could account for the thinning rate derived from the satellite altimetry (Mayer et al., 2018). This is consistent with findings elsewhere in Greenland where the incursion of warm Atlantic waters to outlet glacier margins over the last few decades, as well as increased air temperatures and sea-ice loss, have all been linked to ice margin instability and rapid groundling line retreat (Vieli and Nick, 2011; Straneo and Heimbach, 2013; Khan et al., 2015; Mouginot et al., 2015).

If AIW is circulating throughout the cavity beneath the floating portion of the 79N Glacier then this should have profound consequences for stability of the grounding line (An et al., 2021) and the ice shelf. However, future change depends on cavity geometry and the flux, extent, properties and interaction of AIW with the floating ice and the grounding line (Wilson and Straneo, 2015; Schaffer et al., 2017; Lindeman et al., 2020; Schaffer et al., 2020; An et al., 2021; von Albedyll et al., 2021). Given the clear importance of AIW in controlling the dynamics and stability of 79N glacier it is crucial to understand if it reaches the grounding line and to characterise 79N changes and any links to AIW, across multiple timescales (Lindeman et al., 2020; von Albedyll et al., 2021). Here we report the first empirical evidence for AIW proximal to the grounding line of the 79N Glacier based on CTD measurements in Blåsø, an epishelf lake, located >50 km upstream from the calving front. These are combined with tidal observations, hydrostatic analysis of the ice shelf, synthetic Aperture Radar Interferometry (InSAR) and airborne ice-penetrating radar data in order to characterise contemporary conditions around the grounding line of the ice shelf.

2 Study Area

Epishelf lakes occur between ice-free land areas and ice masses floating on the ocean. Where a source of freshwater feeds into the lake a salinity-driven stratification forms with the more saline marine layer capped by a freshwater layer. The depth of the transition between marine and brackish/fresh water is controlled by the draught of the floating ice, provided it is in hydrostatic equilibrium (Hattersley-Smith, 1973; Gibson and Andersen, 2002). Epishelf lakes are tidal and can contain mixed biological assemblages of marine, brackish and freshwater organisms. They are well known in polar regions and are a particularly rich source of information on the adjacent floating ice margins. For example, epishelf lakes in West Antarctica (Bentley et al., 2005; Smith et al., 2006), East Antarctica (Wagner et al., 2004; Gibson and Andersen, 2002) and the Canadian Arctic (Mueller et al., 2003; Antoniades et al., 2011; Hamilton et al., 2017) have been used to infer past glaciological change such as ice shelf collapse and thickness changes of the floating ice.

https://doi.org/10.5194/tc-2022-206
Preprint. Discussion started: 1 November 2022

Blåsø is an epishelf lake located adjacent to the northern margin of the floating portion of 79N Glacier. The lake is broadly triangular in planform with the two southern apexes of Blåsø in contact with two calving margins (west and east), separated by ~10 km (Fig 1). The northern apex of the lake receives freshwater from a glacier-fed river draining from the north-west, which forms a large prograding delta.

The shoreline of Blåsø has been used to reconstruct past glacier behaviour, with the remains of marine organisms providing clear evidence for retreat of the floating portion of 79N Glacier and marine inundation of the basin during the Holocene Thermal Maximum (8.0-5.0 ka BP; Bennike and Weidick, 2001). Lake core evidence has also been recently used to constrain ice shelf re-advance and epishelf lake reformation to *c.* 4.4 ka BP (Smith et al., submitted).

Multiple approximations for the location of the 79N grounding line have been produced over recent years (Morlighem et al., 2017; ESA Greenland IceSheet CCI, 2017, Mayer et al., 2018) and they are for the most part in general agreement, with the exception of the western calving margin in Blåsø (Fig 1a). Morlighem et al. (2017) (Fig. 1a) and An et al. (2021) suggest that the grounding line has retreated beyond the western margin of Blåsø, so the ice entering the lake is either floating, or very close to it. The other studies indicate that the western end of Blåsø is located somewhere between 1 km and 7 km from the cross-fjord (NW-SE oriented) grounding line with the ice reaching flotation in water depths between 175 m and 450 m. None of the above studies have identified grounding lines along the lateral margins of the ice stream with the exception of the Midgardsormen ridge identified by Mayer et al. (2018) which lies between the western and eastern calving margins of Blåsø.

3 Methods

As part of a wider programme to characterise and sample water and sediments in Blåsø, to understand past changes in the 79N Glacier, the bathymetry of the lake was mapped and multiple CTD profiles were measured in different parts of the lake.

Fieldwork was undertaken at Blåsø between 19th July and 11th August 2017, overlapping with the end of the period of data collection of the ITM reported by Lindeman et al. (2020). We conducted a CHIRP (Compressed High Intensity Radar Pulse) sub-bottom survey to construct a bathymetric map of the lake. The survey was conducted using a SyQuest Bath2010PC sub-bottom profiling unit coupled to a 10 KHz SyQuest P02590-1 transducer. Depth differences at crossovers of survey tracks average 1.6 m but range between -3 and 4.7 m.

CTD profiles were measured with a *Valeport* MiniCTD rated to 500 m with a pressure-balanced conductivity cell, 50 bar strain gauge pressure sensor, and a Platinum Resistance Thermometer sensor. We used the *Datalog X2* software package to record and manipulate CTD data. Manufacturer-cited accuracy was ±0.01 mS/cm, ±0.01 °C, and ±0.05% for pressure. The CTD was factory-calibrated two months before the measurements reported here. The CTD operated continuously and was deployed using a hand-spooled winch from a small boat at eight sites across the lake, with the objective of characterising water conditions at both calving fronts and in the three lake basins identified by the CHIRP survey (Fig 1; Table 1). The CTDs were sampled between 31st July and 10th August 2017 and during this period there was persistent lake ice which prevented CTD measurements close to the eastern calving front. In contrast, most of the lake ice in the western basin had dispersed and melted by early August, allowing access to the western calving margin. Temperature and salinity observations are reported as Conservative Temperature and Absolute Salinity (McDougall & Barker, 2011).

https://doi.org/10.5194/tc-2022-206
Preprint. Discussion started: 1 November 2022

Over several weeks a *VanWalt* LevelSCOUT water pressure transducer was used to measure any tidal variation within the lake. This uses a silicon strain gauge to measure water pressure variations, with a manufacturer-cited accuracy of 0.05% full scale (FS) and a resolution of 0.0034% FS. Water pressure variations were corrected for barometric (atmospheric pressure) variations using measurements from a *VanWalt* BaroSCOUT instrument and the *Aqua4Plus* software package. The LevelSCOUT was secured to a stake submerged in the western end of the lake, and the BaroSCOUT was secured to a stake on the lakeshore <50 m away. Overnight on 28/29th July 2017 the tidal pressure transducer stake was impacted by windblown lake ice floes. The transducer continued to record tidal information but with anomalously high water depth readings due to the tilted stake. On 2nd August the lake ice had moved and the stake was re-positioned to the vertical at the same site. The tidal measurements are therefore presented as three measurement intervals: Interval 1 (25th July – 29th July), Interval 2 (29th July – 2nd August), and Interval 3 (2nd August– 12th August) (Fig. 2). These intervals do not have a common datum and so are not directly comparable in absolute elevation, but the amplitude and period measurements are comparable across the three intervals. The low tide minima between 10-12 August are not fully recorded in the dataset due to sub-aerial exposure of the re-positioned sensor at the lowest tides.

We used three independent approaches to determine the patterns of floating and grounded ice at the calving margins in Blåsø, namely hydrostatic analysis, satellite-derived Synthetic Aperture Radar Interferometry, and airborne radio echo sounding data.

Hydrostatic analysis used the Arctic DEM (Porter et al., 2018) for surface elevations and mapping, BedMachine v3 (Morlighem et al., 2017) for the sub-shelf bathymetry and subglacial topography, our CHIRP survey for lake bathymetry, and the MEaSUREs Greenland Ice Sheet Velocity Map (Joughin et al., 2016; 2017) for surface velocites. Elevations from the Arctic DEM were corrected to orthometric heights using the EIGEN-6C4 geoid from BedMachine v3 (Morlighem et al., 2017). An approximation for the ice shelf thickness, where it is in hydrostatic equilibrium i.e. the ice surface elevation is a direct measure of the local ice thickness, was made using an ice density of 917 kgm^{-3} and sub-shelf water density of 1023 kgm^{-3} (following Morlighem et al., 2017). This was also used to approximate the location of grounded, partially grounded, and floating ice.

We applied Synthetic Aperture Radar Interferometry (InSAR) on Sentinel-1 TOPS SAR data captured on 3, 9, and 15 April 2017. Interferograms are formed from interferometric wide-swath single-look complex data acquired at times t1 and t2 separated by a temporal baseline of 6 days. Assuming constant horizontal ice flow within a 6-day time period we subtracted another interferogram with data acquired at times t2 and t3 to isolate vertical displacements due to ocean tides. Areas of scatter (low coherence) on the interferograms represent areas of ice shelf bending close to grounded ice. Full processing details can be found in Christmann et al. (2021).

We used airborne ice-penetrating radar data to examine the relationship between grounded and floating ice at the eastern calving margin in Blåsø. The data were from the Alfred Wegener Institute (AWI) multi-frequency ultra-wideband (UWB) radar. This is a modified version of the Multichannel Coherent Radar Depth Sounder (MCoRDS), that is mounted on the *Polar 6* Basler BT-67 aircraft. A laserscanner continuously records the elevation of the ice surface in a swath beneath the aircraft. Acquisition parameters can be found in Franke et al (2020) and data were collected on 14th April 2018, approximately 8 months after the field measurements undertaken in Blåsø.

4 Results

https://doi.org/10.5194/tc-2022-206
Preprint. Discussion started: 1 November 2022

Blåsø has an area of 60.7 km^2 and 53.5 km of shoreline. The bathymetric survey of the lake reveals a western basin (maximum depth ~135 m) in front of the west calving front, a central basin (~90 m deep) and an eastern basin (maximum measured depth ~212 m) close to the east calving front (Figure 1b). The central and eastern basins are separated by a broad sill at 57 m depth in the central part of the lake. The western basin is separated from the central basin by a sill at 21 m depth (Fig. 1b) that is consistent with the continuation of a subaerial moraine visible on the western shore. The north-western parts of the lake are very shallow (<20 m) and are occupied by the lower reaches of a large delta. The central basin has a flat floor in which the CHIRP identified stratified sediment.

Figure 1b shows the location of the *VanWalt* LevelSCOUT water pressure transducer. Despite the complications due to the transducer being impacted by an ice floe, the data clearly demonstrate that the lake experiences a semi-diurnal tidal cycle. The maximum tidal range of ~1.2 m (Fig. 2) was only fully recorded during Interval 1. The second half of Interval 2 and the early part of Interval 3 record have the lowest tidal range of ~40 cm. Spring and neap tides were captured within the record.

We obtained eight CTD profiles in Blåsø (Fig. 1, Fig. 3, Table 1). These ranged from 15 m depth around shallow margins of the central basin to 192 m depth in the eastern basin. The deepest profiles were retrieved close to the eastern end of the lake where the CHIRP bathymetry shows the lake deepens significantly towards the calving front. In the western basin CTDs were obtained at a maximum depth of 136 m, immediately adjacent to the calving front.

The profiles show a stratified water column, marked by two prominent haloclines and accompanying thermoclines. We identify four primary water masses within the lake (Figures 3, 4a). The surface layer is a shallow freshwater cap (identified here as water mass 1; salinity <1 to 2 gkg^{-1}), which is approximately 20 m thick. The surface is cooler in the eastern basin (2.3-2.7 °C), where persistent lake ice also trapped a large volume of icebergs, than in the western basin (3.1-4.5 °C) where little lake ice remained into August. Surface temperature also varied with distance from the calving front within the western basin: the profiles CTD3 and CTD4 show warmer surface temperatures than CTD6 and CTD7 that were taken within 100 m of the calving front (Fig. 1b, Fig. 3).

Below water mass 1 is an intermediate brackish layer occupying a depth range from 20 m to 145 m. Properties of this layer vary between the west and east basins. In the eastern basin, salinities are in the range of 5 to 7 g/kg and temperatures 0.5 to 0.8 °C and this is identified as water mass 2. In the western basin, the layer is more saline (11-13 g/kg) and colder (-0.1 to -0.5 °C) and is identified as water mass 3.

Present only in the eastern basin is a seawater layer (water mass 4) which extends to the deepest part of the lake sampled (192 m). Water mass 4 is relatively warm and salty, with temperatures between 0.1 and 0.7 °C and salinity 34.4 to 34.7 g/kg. The lower halocline shows an offset in measured depth of ~5 m between CTD5 and CTD8 in the eastern basin.

During bathymetric and CTD surveys we observed dying fish on the surface of the lake on several occasions. These were only seen in the western basin, close to the calving front, and above the deepest point. The fish were Arctic cod (*Arctogadus glacialis*), a marine fish that is known to live in close proximity to ice (Froese and Pauly, 2021).

Our three approaches to determining the distribution of floating and grounded ice yield slightly different results, with both the interferometry and radio-echo sounding data suggesting that much of the eastern calving margin is floating, but hydrostatic analysis suggesting a narrow grounded zone exists close to the calving front (Figs. 5, 6, 7)

https://doi.org/10.5194/tc-2022-206
Preprint. Discussion started: 1 November 2022

Our new hydrostatically-based estimate for the grounding line has been made across the width of 79N Glacier and at both of the calving margins which enter Blåsø, and these have been tied, as far as is possible, to the CHIRP bathymetry surveys (Fig. 5). The grounding line across most of the fjord is in general agreement with the previous work (Fig. 1a). The location of the grounding line around the western entrance into Blåsø is more complex to interpret. Between 1994 and 2014 Midgardsomen has migrated towards the ice shelf margin (~2 km), and down flow from the entry into the western calving margin of Blåsø (Mayer et al., 2018). The ice sheet/shelf surface slope transition, observed in the Arctic DEM, appears to be located up-flow from the western entry to Blåsø. These observations support the interpretation of Morlighem et al. (2017) (Fig. 1a) and An et al. (2021) that the across-fjord portion of the grounding line is located up-flow of Blåsø (Fig. 5d) and the ice flowing into the western entry of Blåsø is floating. However, the ice surface elevation, taken from the Arctic DEM, suggests that the ice is mostly grounded across the full width of the western margin of Blåsø i.e. the ice is higher than it should be if the ice were free floating(Fig. 5d). The data are equivocal so two possible locations for the grounding line are shown on Figure 5 with the most likely scenario being that the ice is only partially grounded in the area between the two dashed lines (Fig. 5) as indicated in Figure 5d.

The hydrostatic analysis suggests that much of the ice draining into the eastern end of Blåsø appears to be grounded, due to the ice surface elevation being greater than that required for the ice to be floating and in hydrostatic equilibrium. This is supported by the presence of the Midgardsormen ridge (Mayer et al., 2018), which runs along the northwestern margin of the ice shelf and across the eastern entry into Blåsø (Fig. 5e). There is, however, an area of floating ice that extends west from Midgardsomen and reaches to within 300 m of the eastern calving front in Blåsø (Fig. 5c). Figure 5 shows profiles across the eastern calving front with one oriented along the deepest centre-line of the eastern basin of Blåsø (Fig 5e) and a second aligned through the area of floating ice closest to the calving front and which terminates on the shallower (~50 m depth) southern flank of the eastern basin (Fig 5f).

We are able to further resolve the extent of grounded and floating ice at the two calving fronts in Blåsø using interferometric analysis (Fig 6). Double differential interferograms from data captured on 3, 9 and 15 April 2017 help demonstrate the extent of grounded and floating ice. At the western calving margin the band of fringes showing grounded ice extends across the calving front. At its narrowest this grounded ice only extends a few 100m behind the calving front (Fig 6a). A small ice rise (grounded ice within the floating ice shelf) is evident ~3 km to the south of the calving front. A double differential interferogram of the eastern calving front provides a more detailed view than the hydrostatic analysis and shows that unlike the western margin the calving front is not grounded (Fig 6b) over most of its area. A small ice rise and narrow zone of possible grounding along the Midgardsormen is evident 1-2 km behind the calving front.

Our third approach, using ice radar data, shows that the eastern margin is actually floating on both sides of Midgardsormen (Fig. 7). A prominent reflector shows the ice shelf base with a draught in the lake of approximately 150m (Fig 7a) immediately behind the calving front. The laser scanner data show the ice surface to be higher at the location where interferometry suggests an ice rise exists (Fig 7b).

5 Discussion

Recent studies have suggested that thinning of the 79N Glacier ice tongue near the grounding line over the past two decades has been driven primarily by warming of ocean waters within the cavity (Mouginot et al., 2015; Mayer et al., 2018; Schaffer et al., 2020; Lindeman et al., 2020). However, this warming has been inferred from limited observations in the vicinity of the calving front, over 70 km away from the grounding line, due to the difficulty of accessing the sub-

https://doi.org/10.5194/tc-2022-206
Preprint. Discussion started: 1 November 2022

shelf cavity. The data presented here demonstrate that the seawater properties observed between 160 m and 193 m in the eastern basin of Blåsø lie on a melt-mixing line between the properties of melt-modified AIW recorded by the ITM deployed in the rift of the ice shelf near the calving margin in July 2017 at 150 m and 250 m (Figure 4b; Toole et al., 2016). This provides the first direct evidence that warm AIW is circulating deep within the sub-ice shelf cavity, and reaching proximal to the grounding line of 79N glacier. The CTD observations made in Blåsø, some 50 km inboard of the calving front appear to reflect conditions recorded by the ITM proximal to the calving front.

Lindeman et al. (2020) show that trends in the AIW inflow properties at the ITM, observed at 500 m depth, are reflected in the exported melt-modified waters at 250 m with a lag of approximately 6 months, i.e., properties at 250 m in July 2017 fall along a melt mixing line relative to 500 m properties in January 2017. In the eastern basin of Blasø in August 2017 (CTD 8), T-S properties below 175 m fall along the same mixing line (Figure 4b). This indicates that variability in AIW inflow properties, observed near the calving front, propagates into the sub-ice shelf cavity, to within 20-30 km of, and likely all the way to (see Schaffer et al. 2020, Fig. 4), the grounding line, in <7 months. Flow of melt-modified AIW from the continental shelf to the grounding line is consistent with the conclusions of Wilson and Straneo (2015) and Schaffer et al. (2020), who calculated the residence times for water in the ice shelf cavity as 110-320 days and 162 days respectively. The data presented here lie within this range and further constrain this transmission.

The water pressure transducer data demonstrate clearly that Blåsø is tidal, confirming connection to the ocean. The tides recorded in Blåsø are consistent with the frequency and range of tidal measurements made by Reeh et al (2000) in open water close to Bloch Nunatakker (referred to as “Syge Moster” in Reeh et al.) at the calving front of the floating tongue of 79N in 1997 (Reeh et al., 2000) (Fig. 1a). The 1997 measurements were recorded only for a few days but themselves are similar to the tidal measurements at the Danmarkshavn tide gauge (76° 46’ N, 18° 46’ W; Fig. 1a) with a lead of approximately 50 minutes at Bloch Nunatakker. Reeh et al. (2000) also measured tidal motion of the ice shelf itself using GPS receivers along a cross-glacier profile a few kilometres east of Blåsø. The tidal motion of the ice shelf leads the tidal cycle by ~65 minutes and has a tidal amplitude ~75% of that measured at Danmarkshavn (Reeh et al., 2000). The tidal signal recorded in Blåsø shows a lead of ~1 hour and a tidal amplitude ~65% of that recorded at Danmarkshavn (Fig. 2) consistent with the measurements made by Reeh et al. (2000). The slightly reduced tidal amplitude measured in Blåsø compared to that measured by Reeh et al. (2000), in relation to the Danmarkshavn record, may indicate that the tidal flow into and out of Blåsø is somewhat restricted supporting the evidence presented above, that ice flowing into both the western and eastern basins of Blåsø is partially grounded (Fig. 5-7).

CTD data show two haloclines in the lake. The 20 m surface layer likely represents a combination of surface heating and the presence of a lake floor moraine which acts as a sill at 21 m depth preventing exchange of deeper water from the western basin into the central basin. The halocline at 145 m acts as a proxy for the draught of the floating tongue of 79N Glacier at the eastern margin if the ice were in hydrostatic equilibrium. In waters shallower than this the freshwater runoff from the catchment and the surface of the ice shelf is impounded by the calving cliffs. Deeper than this there is tidal exchange of seawater that comes from under the floating tongue of 79N Glacier.

The difference of ~5 m between the depths of the lower halocline measured in CTD5 and CTD8 (Fig. 2) cannot be explained by barotropic tidal variation (1.2m) alone. CTD5 was sampled on 7th August close to low tide, whilst CTD8 was sampled on 10th August, 1 hour after high tide. It is more likely that the difference is caused by internal waves which can be created where tidal currents drive water parcels, especially, on steep slopes (Munk and Warren, 1981). Our newly-measured bathymetry presented here shows that the lake deepens rapidly in its eastern end with a slope from the central sill towards the eastern calving front. Such slopes, along with a tidal forcing, are conducive to the

https://doi.org/10.5194/tc-2022-206
Preprint. Discussion started: 1 November 2022

development of internal waves along boundaries between water layers of different density, as seen in the eastern basin. Internal waves are of significantly larger amplitude than any surface expression, and move more slowly (Sverdrup et al., 1942). Hence the offset between CTD5 and CTD8 may be the result of an internal wave propagated through the eastern basin. Such waves have been shown to drive high frequency variability in halocline depth at the Milne Fiord epishelf lake in the Canadian Arctic (Hamilton et al., 2017).

BedMachine infers a steep slope on the side of the fjord under the 79N ice shelf (Fig. 6), but we note some of the limitations of inferring bathymetry beneath floating ice. The ice surface elevation and the Midgardsormen-defined grounding line (Fig. 5, 6b, 6c) indicate that much of the ice flowing into the eastern basin is grounded along the fjord side, but the 145 m-depth halocline is close to the draught of the floating part of the ice shelf, on both sides of where it is grounded at the Midgardsormen (Fig 7a). CTD5 and CTD8 demonstrate a direct connection to the sub-shelf water circulation and data from the *VanWalt* LevelSCOUT water pressure transducer imply that there is unencumbered tidal exchange of seawater between the lake and the sub-shelf cavity. The interferometric analysis and radar data show this floating ice at the eastern margin clearly (Fig 6b, Fig 7a) and demonstrate an ice shelf draught of approximately 150m, consistent with the halocline measured at CTD5 and CTD8. The difference in patterns of grounded and floating ice between the interferometric and radar datasets on the one hand and the hydrostatic analysis on the other, suggest that the lower resolution of the hydrostatic analysis may fail to capture smaller-scale detail of the bed or that it is perhaps affected by the areas of local grounding demarcated by the interferometry, and which may allow the ice to be supported at higher elevations, or 'bridged' between grounded areas.

It is also likely that hydrostatic analysis would not pick up areas of local floating ice such as associated with sub-ice channels below the resolution of the data used in hydrostatic analysis. The Midgardsormen splits as it bends slightly into the eastern margin of Blåsø, mirroring an embayment in the fjord bathymetry (Fig. 5 inset). This is interpreted to represent the most likely location of the connection between the deeper parts of the lake and the sub-ice shelf environment. In later imagery from 2020 (Fig. 1b), it appears that the Midgardsormen has migrated farther landward as the ice shelf thinned, suggesting that the connection between the eastern basin and the sub-ice shelf cavity may only recently have been created or has enlarged in recent years.

Our observations of brackish water and dying fish show that there is also some connection between the ocean waters and this epishelf lake at the western margin. As there is no seawater present in the deepest parts of the western basin, this implies that the seawater layer in the sub-shelf cavity lies deeper than the lake bed (136 m at CTD 7). This is consistent with either of the dashed grounding lines shown in Figure 5. However, the salinities of >10 gkg^{-1} in water mass 3 implies that there has been some recent mixing of lake water with seawater. The observations of dying marine fish at the surface of the western basin is further compelling evidence of an ongoing marine connection. The assumption is that marine fish present in the seawater under the ice shelf are transported into the lowermost brackish parts of the western basin, and float to the surface when their salt balance and buoyancy are disrupted due to osmotic lysis. The most likely explanation is that the ice is only partially grounded between the fjord and the western calving front. Spring tides, internal waves or flow of buoyant sub-ice shelf meltwater could create a mechanism that pumps seawater (and fish) sporadically beneath the partially grounded ice into the deepest part of the western basin. The interferometric analysis shows that at its narrowest the zone of grounded ice at the western margin is only a few 100 m wide and it is possible that local thinning or sub-ice channels may allow seawater to enter the lake.

Analysis of the margins and marine connections in both the western and eastern basins clearly indicate that the ice shelf margin has thinned sufficiently to begin un-grounding and allow the ingress of marine water into Blåsø. This represents

https://doi.org/10.5194/tc-2022-206
Preprint. Discussion started: 1 November 2022

a critical process in the retreat of a marine-terminating glacier such as 79N. Continued thinning would lead to complete ungrounding and penetration of warmer marine waters into shallower parts of Blåsø marking its transition to a fully marine basin, analogous to its configuration during the early Holocene (Bennike and Weidick, 2001; Smith et al., submitted).

6 Conclusions

The measurements reported here provide the first measurement of melt-modified Atlantic Intermediate Water (AIW) immediately proximal to the grounding line of Nioghalvfjerdsfjorden (79N) Glacier. Measurements show that the water below 145 m depth in the eastern basin of Blåsø has very similar properties to, and lies on the mixing line of, AIW measured some months previously in a rift mooring ~50 km away (Lindeman et al., 2020). Our observations also show that the transit time from close to the front of the floating ice tongue to Blåsø is of the order of <7 months.

We show that different approaches to determining patterns of floating and grounded ice at the margin of the ice shelf can yield significant differences, with ice radar and interferometry yielding a more consistent pattern than hydrostatic analysis, where patterns are likely complicated by local bed and ice shelf base topography, and potential stress bridging.

Recent studies have emphasised the importance of monitoring water mass properties entering the 79N Glacier sub-ice shelf cavity and understanding the associated circulation (e.g. Lindeman et al., 2020; Schaffer et al., 2020). This study shows that melt-modified AIW is present in the eastern basin of Blåsø, at depths >145 m, and therefore must be present under the adjacent ice shelf. Our observations are from a location where ocean variability and the grounding line evolution could be relatively easily monitored. Monitoring the intrusion of AIW beneath the ice shelf, including changes to the water mass properties, may be possible by future installation of oceanographic moorings in Blåsø, ideally in both the western and eastern basins. Combined with observations of AIW changes outside the ice shelf, this would allow continuous monitoring of their propagation into the cavity toward the grounding line of the largest ice stream in Greenland, potentially revealing variability in circulation and susceptibility of ice tongue melt to ocean warming. Such oceanographic measurements close to grounding lines are normally only possible by sporadic drilling through ice tongues or ice shelves which are high cost and logistically difficult. Continuous CTD monitoring in the western basin would identify the further un-grounding as the margin thins to a critical thickness that will allow the establishment of a permanent connection between the western basin and the sub-ice shelf cavity.

The observation of melt-modified AIW proximal to the grounding line has significant implications for the 79N Glacier because basal melting is critical to its stability (Mouginot et al., 2015; Schaffer et al., 2017; An et al., 2021). Our observations confirm modelling studies that have assumed circulation of AIW throughout the entirety of the cavity beneath the 79N Glacier floating tongue, whilst being mixed with (basal) melt from the glacier. Future modelling of 79N Glacier evolution can use these observations to constrain water mass properties at the grounding line of this glacier which drains 6.28% of the Greenland Ice Sheet (Krieger et al., 2020). Our data on the circulation times within the cavity provide an empirical constraint on how quickly warming of the AIW, that has been observed on the continental shelf, is transmitted to the grounding line of 79N Glacier (Wilson and Straneo, 2015; Schaffer et al., 2017; Schaffer et al., 2020).

Data Availability

CTD data and pressure transducer data from Blåsø are available from the UK NERC Polar Data Centre (http://www.bas.ac.uk/data/uk-pdc/) *[data have been submitted but awaiting the two dois to be minted]*.

https://doi.org/10.5194/tc-2022-206
Preprint. Discussion started: 1 November 2022

390 **Author contributions**

MB, DR, JS, JL conceptualised the epishelf lake measurements. MB, JS, SJ undertook field measurements in Blåsø aided by CD, DR, TL whilst ML, FS were responsible for collection and interpretation of sub-ice shelf mooring data. AH and VH collected and analysed airborne radar and satellite interferometric data. MB analysed pressure transducer data and BR undertook hydrostatic analysis. All authors contributed to data interpretation. MB led writing of the
395 manuscript with DR, BR, and all authors commented on the manuscript.

Competing interests

The authors declare that they have no conflict of interest.

Acknowledgements

This work was carried out as part of UK NERC Grant, NE/N011228/1 'Greenland in a warmer climate: What controls
400 the advance & retreat of the NE Greenland Ice Stream'. We thank the Alfred Wegner Institute, in particular Hicham Rafiq, for their significant logistic support through the iGRIFF project to the work reported here. The airborne data were acquired as part of the campaign RESURV79 conducted by Polar 6. We also thank Jorgen Skafte (Villum Research Station), Nordland Air, Air Greenland, Joint Arctic Command (Station Nord) and Nanu-Travel (in particular Isak and Ooni) for their role in supporting the fieldwork at Blåsø. Naalakkersuisut, Government of Greenland, provided
405 Scientific Survey (VU-00121) and Export (046/2017) licences for this work. We also acknowledge help from the Danmarks Meteorologiske Institut for supplying tidal data, and the support of the Department of Geography, Durham University. Chris Orton (Durham Geography) made Figure 5d-f.

References

410 An, L., Rignot, E., Wood, M., Willis, J. K., Mouginot, J., and Khan, S. A.: Ocean melting of the Zachariae Isstrøm and Nioghalvfjerdsfjorden glaciers, northeast Greenland, Proc Natl Acad Sci USA, 118, e2015483118, https://doi.org/10.1073/pnas.2015483118, 2021.

Antoniades, D., Francus, P., Pienitz, R., St-Onge, G., and Vincent, W. F.: Holocene dynamics of the Arctic's largest ice shelf, Proceedings of the National Academy of Sciences, 108, 18899–18904, https://doi.org/10.1073/pnas.1106378108,
415 2011.

Bamber, J. L., Griggs, J. A., Hurkmans, R. T. W. L., Dowdeswell, J. A., Gogineni, S. P., Howat, I., Mouginot, J., Paden, J., Palmer, S., Rignot, E., and Steinhage, D.: A new bed elevation dataset for Greenland, The Cryosphere, 7, 499–510, https://doi.org/10.5194/tc-7-499-2013, 2013.

Bennike, O. and Weidick, A.: Late Quaternary history around Nioghalvfjerdsfjorden and Jøkelbugten, North-East
420 Greenland, 30, 205–227, https://doi.org/10.1111/j.1502-3885.2001.tb01223.x, 2008.

Bentley, M. J., Hodgson, D. A., Sugden, D. E., Roberts, S. J., Smith, J. A., Leng, M. J., and Bryant, C.: Early Holocene retreat of the George VI Ice Shelf, Antarctic Peninsula, Geol, 33, 173, https://doi.org/10.1130/G21203.1, 2005.

Beszczynska-Möller, A., Fahrbach, E., Schauer, U., and Hansen, E.: Variability in Atlantic water temperature and transport at the entrance to the Arctic Ocean, 1997–2010, 69, 852–863, https://doi.org/10.1093/icesjms/fss056, 2012.

425 Christmann, J., Helm, V., Khan, S.A. et al. Elastic deformation plays a non-negligible role in Greenland's outlet glacier flow. Commun Earth Environ 2, 232 (2021). doi.org/10.1038/s43247-021-00296-3.

Dicks, L.: Arctic Climate Issues 2011: changes in Arctic snow, water, ice and permafrost. SWIPA 2011 Overview report, Arctic Monitoring and Assessment Programme, AMAP, Oslo, 97 pp., 2012.

ESA Greenland_Icesheet_CCI, Grounding Lines from SAR Interferometry: ESA Greenland_Icesheet_CCI, Grounding
430 Lines from SAR Interferometry, http://products.esa-icesheets-cci.org/products/details/greenland_grounding_line_locations_v1_3.zip/, 2017.

Franke S, Jansen D, Binder T, Dörr N, Helm V, Paden J, Steinhage D, Eisen O. Bed topography and subglacial landforms in the onset region of the Northeast Greenland Ice Stream. Annals of Glaciology 61 (81), 143–153. https://doi.org/10.1017/aog.2020.12

435 Froese, R. and Pauly, D. (Eds.): FishBase, www.fishbase.org, 2021.

Gibson, J. A. E. and Andersen, D. T.: Physical structure of epishelf lakes of the southern Bunger Hills, East Antarctica, Antartic science, 14, 253–261, https://doi.org/10.1017/S095410200200010X, 2002.

Hamilton, A. K., Laval, B. E., Mueller, D. R., Vincent, W. F., and Copland, L.: Dynamic response of an Arctic epishelf lake to seasonal and long-term forcing: implications for ice shelf thickness, The Cryosphere, 11, 2189–2211,
440 https://doi.org/10.5194/tc-11-2189-2017, 2017.

Hanna, E., Cappelen, J., Fettweis, X., Mernild, S. H., Mote, T. L., Mottram, R., Steffen, K., Ballinger, T. J., and Hall, R. J.: Greenland surface air temperature changes from 1981 to 2019 and implications for ice-sheet melt and mass-balance change, Int J Climatol, 41, https://doi.org/10.1002/joc.6771, 2021.

Hattersley-Smith, G.: Ice Shelf and Fiord Ice Problems in Disraeli Fiord Northern Ellesmere Island, NWT., Defence
445 Research Establishment Ottawa Tech. Note, 72-34, 1972.

Humbert, A., Helm, V., Neckel, N., Zeising, O., Rückamp, M., Khan, S. A., Loebel, E., Gross, D., Sondershaus, R., and Müller, R.: Precursor of disintegration of Greenland's largest floating ice tongue, The Cryosphere Discuss. [preprint], https://doi.org/10.5194/tc-2022-171 , in review, 2022.

Joughin, I., Smith, B., Howat, I., and Scambos, T.: MEaSUREs Multi-year Greenland Ice Sheet Velocity Mosaic,
450 Version 1., Version 1, https://doi.org/10.5067/QUA5Q9SVMSJG, 2016 [Last accessed December 2021].

Joughin, I., Smith, B. E., and Howat, I. M.: A complete map of Greenland ice velocity derived from satellite data collected over 20 years, J. Glaciol., 64, 1–11, https://doi.org/10.1017/jog.2017.73, 2018.

Khan, S. A., Kjær, K. H., Bevis, M., Bamber, J. L., Wahr, J., Kjeldsen, K. K., Bjørk, A. A., Korsgaard, N. J., Stearns, L. A., van den Broeke, M. R., Liu, L., Larsen, N. K., and Muresan, I. S.: Sustained mass loss of the northeast Greenland
455 ice sheet triggered by regional warming, Nature Climate Change, 4, 292–299, https://doi.org/10.1038/nclimate2161, 2014.

Khan, S. A., Aschwanden, A., Bjørk, A. A., Wahr, J., Kjeldsen, K. K., and Kjær, K. H.: Greenland ice sheet mass balance: a review, Rep. Prog. Phys., 78, 046801, https://doi.org/10.1088/0034-4885/78/4/046801, 2015.

Krieger, L. Floricioiu, D., Neckel, N: Drainage basin delineation for outlet glaciers of Northeast Greenland based on Sentinel-1 ice velocities and TanDEM-X elevations, Remote Sensing of Environment, 237, 111483, https://doi.org/10.1016/j.rse.2019.111483, 2020.

Lindeman, M. R., Straneo, F., Wilson, N. J., Toole, J. M., Krishfield, R. A., Beaird, N. L., Kanzow, T., and Schaffer, J.: Ocean Circulation and Variability Beneath Nioghalvfjerdsbræ (79 North Glacier) Ice Tongue, J. Geophys. Res. Oceans, 125, https://doi.org/10.1029/2020JC016091, 2020.

Mayer, C., Reeh, N., Jung-Rothenhäusler, F., Huybrechts, P., and Oerter, H.: The subglacial cavity and implied dynamics under Nioghalvfjerdsfjorden Glacier, NE-Greenland, Geophys. Res. Lett., 27, 2289–2292, https://doi.org/10.1029/2000GL011514, 2000.

Mayer, C., Schaffer, J., Hattermann, T., Floricioiu, D., Krieger, L., Dodd, P. A., Kanzow, T., Licciulli, C., and Schannwell, C.: Large ice loss variability at Nioghalvfjerdsfjorden Glacier, Northeast-Greenland, Nat Commun, 9, 2768, https://doi.org/10.1038/s41467-018-05180-x, 2018.

McDougall, T. J. and Barker, P. M.: Getting started with TEOS-10 and the Gibbs Seawater (GSW) Oceanographic Toolbox, http://www.teos-10.org/pubs/Getting_Started.pdf, 2011.

Morlighem, M., Williams, C. N., Rignot, E., An, L., Arndt, J. E., Bamber, J. L., Catania, G., Chauché, N., Dowdeswell, J. A., Dorschel, B., Fenty, I., Hogan, K., Howat, I., Hubbard, A., Jakobsson, M., Jordan, T. M., Kjeldsen, K. K., Millan, R., Mayer, L., Mouginot, J., Noël, B. P. Y., O'Cofaigh, C., Palmer, S., Rysgaard, S., Seroussi, H., Siegert, M. J., Slabon, P., Straneo, F., van den Broeke, M. R., Weinrebe, W., Wood, M., and Zinglersen, K. B.: BedMachine v3: Complete Bed Topography and Ocean Bathymetry Mapping of Greenland From Multibeam Echo Sounding Combined With Mass Conservation, Geophys. Res. Lett., 44, https://doi.org/10.1002/2017GL074954, 2017.

Mouginot, J., Rignot, E., Scheuchl, B., Fenty, I., Khazendar, A., Morlighem, M., Buzzi, A., and Paden, J.: Fast retreat of Zachariae Isstrom, northeast Greenland, Science, 350, 1357–1361, https://doi.org/10.1126/science.aac7111, 2015.

Mueller, D. R., Vincent, W. F., and Jeffries, M. O.: Break-up of the largest Arctic ice shelf and associated loss of an epishelf lake, Geophys. Res. Lett., 30, 2003GL017931, https://doi.org/10.1029/2003GL017931, 2003.

Munk, W.: Internal waves and small-scale processes., in: Evolution of Physical Oceanography, MIT Press, , 623, 1981.

Polyakov, I. V., Pnyushkov, A. V., and Timokhov, L. A.: Warming of the Intermediate Atlantic Water of the Arctic Ocean in the 2000s, 25, 8362–8370, https://doi.org/10.1175/JCLI-D-12-00266.1, 2012.

Porter, C., Morin, P., Howat, I., Noh, M.-J., Bates, B., Peterman, K., Keesey, S., Schlenk, M., Gardiner, J., Tomko, K., Willis, M., Kelleher, C., Cloutier, M., Husby, E., Foga, S., Nakamura, H., Platson, M., Wethington, M., Williamson, C., Bauer, G., Enos, J., Arnold, G., Kramer, W., Becker, P., Doshi, A., D'Souza, C., Cummens, P., Laurier, F., and Bojesen, M.: ArcticDEM, https://doi.org/10.7910/DVN/OHHUKH, 2018 [Last accessed December 2021].

Reeh, N., Mayer, C., Olesen, O. B., Christensen, E. L., and Thomsen, H. H.: Tidal movement of Nioghalvfjerdsfjorden glacier, northeast Greenland: observations and modelling, Ann. Glaciol., 31, 111–117, https://doi.org/10.3189/172756400781820408, 2000.

https://doi.org/10.5194/tc-2022-206
Preprint. Discussion started: 1 November 2022

Ribergaard, M. H.: Tidevandstabeller for grønlandske farvande 2017 / Tide tables for Greenlandic waters 2017, Danish Meteorological Institute, Copenhagen, 2017.

Rignot, E.: Rapid Bottom Melting Widespread near Antarctic Ice Sheet Grounding Lines, 296, 2020–2023, https://doi.org/10.1126/science.1070942, 2002.

Schaffer, J., von Appen, W.-J., Dodd, P. A., Hofstede, C., Mayer, C., de Steur, L., and Kanzow, T.: Warm water pathways toward Nioghalvfjerdsfjorden Glacier, Northeast Greenland, J. Geophys. Res. Oceans, 122, 4004–4020, https://doi.org/10.1002/2016JC012462, 2017.

Schaffer, J., Kanzow, T., von Appen, W.-J., von Albedyll, L., Arndt, J. E., and Roberts, D. H.: Bathymetry constrains ocean heat supply to Greenland's largest glacier tongue, Nat. Geosci., 13, 227–231, https://doi.org/10.1038/s41561-019-0529-x, 2020.

Smith, J. A., Hodgson, D. A., Bentley, M. J., Verleyen, E., Leng, M. J., and Roberts, S. J.: Limnology of Two Antarctic Epishelf Lakes and their Potential to Record Periods of Ice Shelf Loss, J Paleolimnol, 35, 373–394, https://doi.org/10.1007/s10933-005-1333-8, 2006.

Smith, J.A., Callard, L., Bentley, M.J., Jamieson, S.S.R., Sánchez-Montes, M.L., Lane, T. P., Lloyd, J.M., McClymont, E. L., Darvill, C., Rea, B.R.., O'Cofaigh, C., Moreton, S.G., Ehrmann, W., and Roberts, D.H. (submitted) Holocene history of 79°N ice shelf reconstructed from epishelf lake and uplifted glacimarine sediments. The Cryosphere.

Stommel, H. M., Warren, B. A., and Wunsch, C. (Eds.): Evolution of physical oceanography: scientific surveys in honor of Henry Stommel, MIT Press, Cambridge, Mass, 623 pp., 1981.

Straneo, F. and Heimbach, P.: North Atlantic warming and the retreat of Greenland's outlet glaciers, Nature, 504, 36–43, https://doi.org/10.1038/nature12854, 2013.

Sverdrup, H. U., Johnson, M. W., and Fleming, R. H.: The Oceans, Their Physics, Chemistry, and General Biology. New York: Prentice-Hall., Prentice Hall, 1942.

Toole, J. M., Krishfield, R., and Woods Hole Oceanographic Institution Ice-Tethered Profiler Program: Oceanographic profile observations collected from station ITM-5 by Woods Hole Oceanographic Institution (WHOI) in the 79 North Glacier, Greenland, from 2016-08-23 to 2018-12-22, https://accession.nodc.noaa.gov/0157557, 2016.

Vieli, A. and Nick, F. M.: Understanding and Modelling Rapid Dynamic Changes of Tidewater Outlet Glaciers: Issues and Implications, Surv Geophys, 32, 437–458, https://doi.org/10.1007/s10712-011-9132-4, 2011.

Von Albedyll, L., Schaffer, J., and Kanzow, T.: Ocean Variability at Greenland's Largest Glacier Tongue Linked to Continental Shelf Circulation, J. Geophys. Res. Oceans, 126, https://doi.org/10.1029/2020JC017080, 2021.

Wagner, B., Cremer, H., Hultzsch, N., Gore, D. B., and Melles, M.: Late Pleistocene and Holocene history of Lake Terrasovoje, Amery Oasis, East Antarctica, and its climatic and environmental implications, Journal of Paleolimnology, 32, 321–339, https://doi.org/10.1007/s10933-004-0143-8, 2004.

Wilson, N. J. and Straneo, F.: Water exchange between the continental shelf and the cavity beneath Nioghalvfjerdsbræ (79 North Glacier), Geophys. Res. Lett., 42, 7648–7654, https://doi.org/10.1002/2015GL064944, 2015.

https://doi.org/10.5194/tc-2022-206
Preprint. Discussion started: 1 November 2022

Yin, J., Overpeck, J. T., Griffies, S. M., Hu, A., Russell, J. L., and Stouffer, R. J.: Different magnitudes of projected subsurface ocean warming around Greenland and Antarctica, Nature Geoscience, 4, 524–528, https://doi.org/10.1038/ngeo1189, 2011.

https://doi.org/10.5194/tc-2022-206
Preprint. Discussion started: 1 November 2022

Figures and Tables

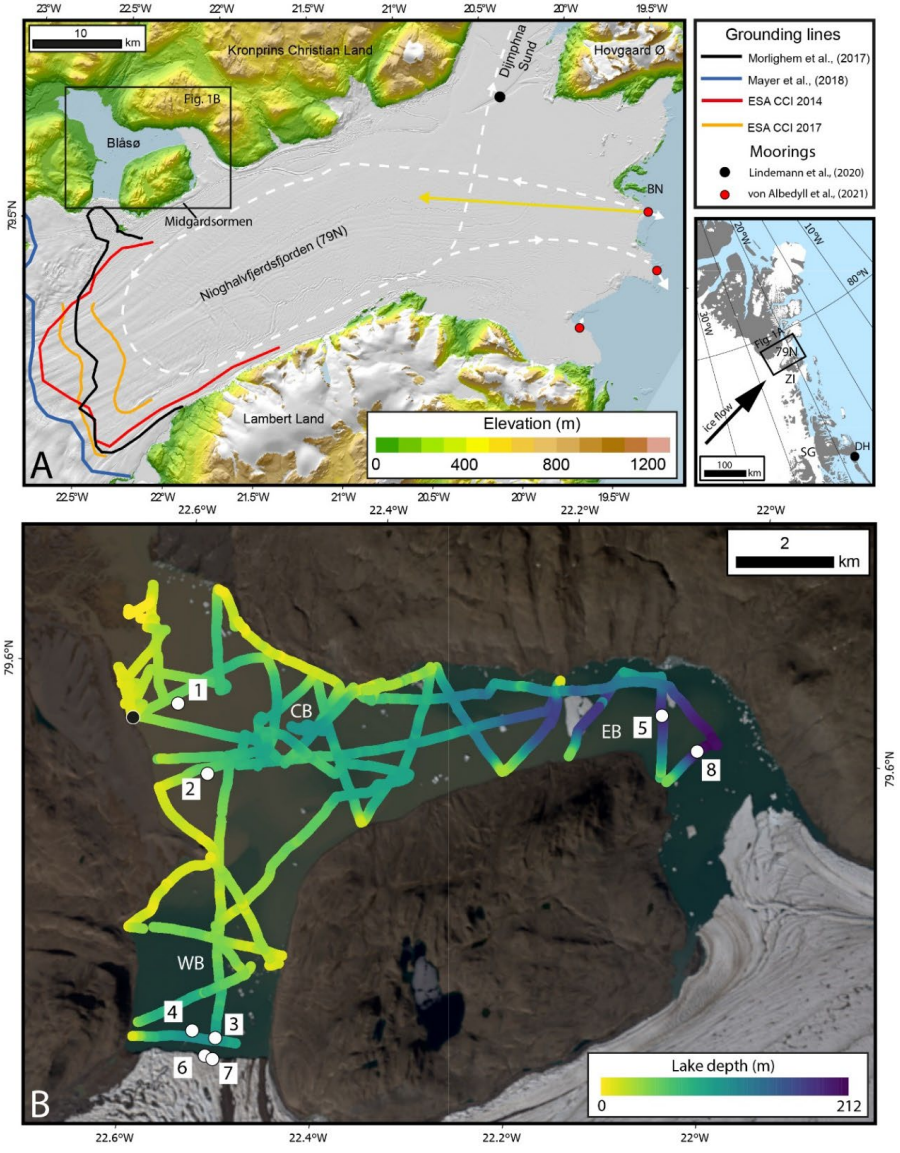

Figure 1. Location Map of Blåsø. **(A)** Nioghalvfjerdsfjorden floating tongue and the location of Blåsø on its northern side, and the 79N grounding line (Mayer et al., 2018; Morlighem et al., 2017; ESA CCI v.1.3) in the context of regional topography from the ArcticDEM (Porter et al., 2018). Black dot marks location of rift mooring of Lindeman et al (2020). BN=Bloch Nunatakker. Red dots show where moorings have measured flow directions in (yellow arrow) and out (white arrows) of the cavity. Arrow lengths are scaled by current speed (von Albedyll et al. 2021). Dashed lines show a potential cavity circulation (von Albedyll et al 2021). Inset shows location of Fig. 1a, ZI = Zachariae Isstrøm, SG =, Storstrømmen Glacier, DH=Dansmarkhavn. **(B)** Blåsø bathymetry and CTD locations. Colour ramp along transect lines shows surveyed water depths using CHIRP and demonstrates the presence of a Western basin (WB), central basin (CB) and Eastern basin (EB) in relation to the western and eastern calving fronts. Locations of numbered

https://doi.org/10.5194/tc-2022-206
Preprint. Discussion started: 1 November 2022


The Cryosphere Discussions
Open Access
EGU

CTD sites are shown as white dots and the tide gauge is shown as a black dot. Satellite image is Landsat 8, from 2nd August 2020. Note that during July-August 2017 the eastern end of the lake S and E of the site of CTD8 was occupied by floating lake ice, the edge of which was close to the bathymetric survey line passing through CTD8 and thus the depth of water at the eastern calving margin is not known.

https://doi.org/10.5194/tc-2022-206
Preprint. Discussion started: 1 November 2022

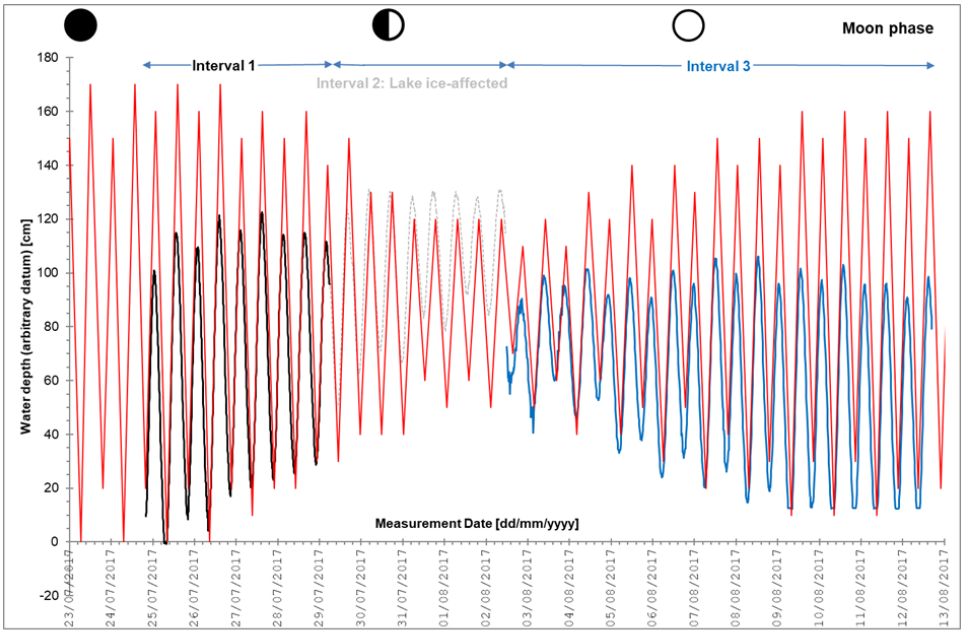

Figure 2. Record of water level fluctuations at Blåsø, 25 July 2017 to 12 August 2017. Intervals 1 (black), 2 (grey) and 3 (blue) are described in the text but intervals 1 and 3 have different (arbitrary) datums; the data in interval 3 have been displaced vertically for plotting to allow approximate comparison with Interval 1. Red line shows tidal data for Dansmarkhan tide gauge (Ribergaard. 2017). Moon phases are shown (New moon - 23/7/17, First quarter - 30/7/17, and Full Moon - 7/8/17). All times are Universal time. The pressure transducer record of water fluctuations demonstrates the semi-diurnal tidal cycle in the Blåsø epishelf lake.

https://doi.org/10.5194/tc-2022-206
Preprint. Discussion started: 1 November 2022

555

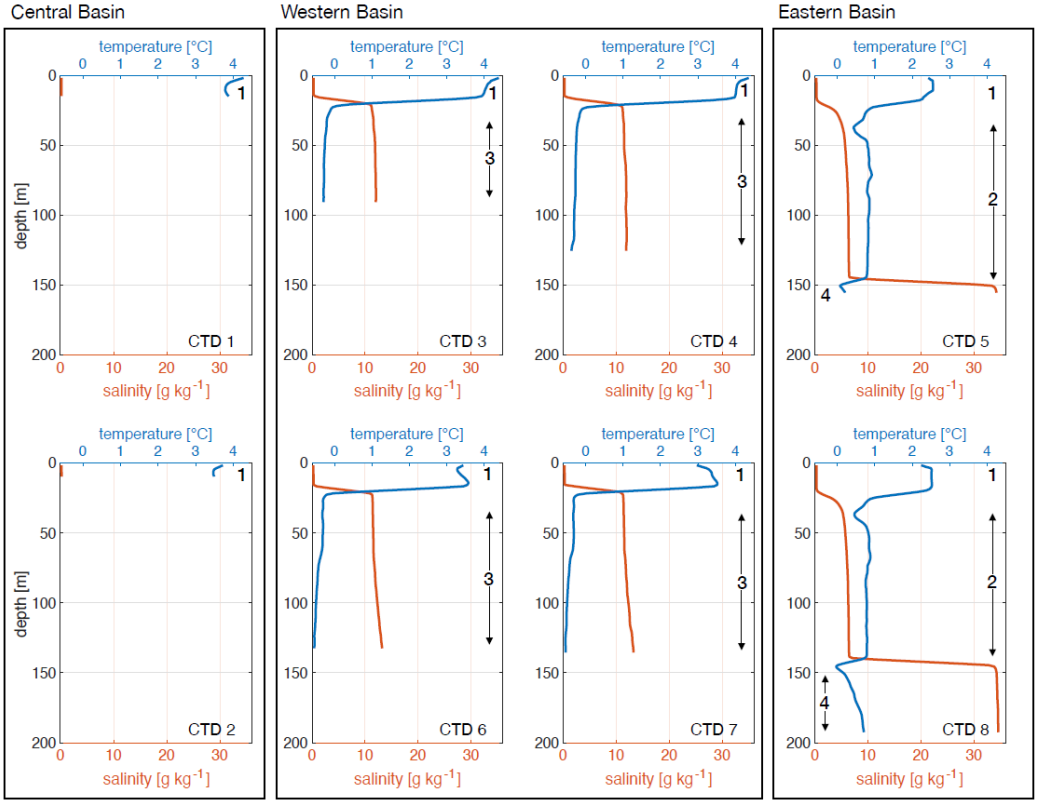

Figure 3. Temperature and salinity profiles observed at locations indicated on Figure 1b and in Table 1, arranged by basin. Bold numbers refer to Water Mass numbers discussed in text.

560

https://doi.org/10.5194/tc-2022-206
Preprint. Discussion started: 1 November 2022

The Cryosphere Discussions
Open Access
EGU

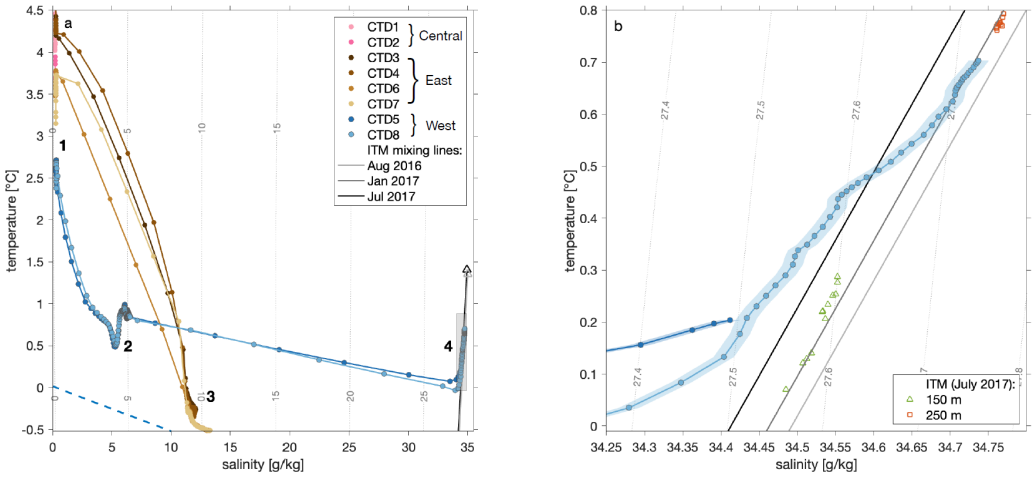

Figure 4. (a) Temperature-salinity plot of the profiles shown in Figure 3. Observations from the eastern basin (CTDs 5 and 8) are in blue. Water masses 1-4, as described in the text, are labelled. The melt mixing lines correspond to the AIW properties observed at 500 m depth in the rift by the ITM in August 2016 (open grey triangle) and July 2017 (open black triangle) (Lindeman et al., 2020). The dashed blue line indicates the surface freezing temperature. Shaded grey box shows extent of Fig 4b.

(b) Temperature-salinity plot of data for water mass 4 between 140 and 193 m depth in the eastern basin, only. The shaded range indicates the instrument accuracy. Melt mixing lines relative to AIW properties at the ITM site are plotted for August 2016 (light grey), January 2017 (dark grey), and July 2017 (black). Daily values of temperature and salinity observed by the ITM are plotted for 150 m (green triangles) and 250 m (red squares) depths.

https://doi.org/10.5194/tc-2022-206
Preprint. Discussion started: 1 November 2022

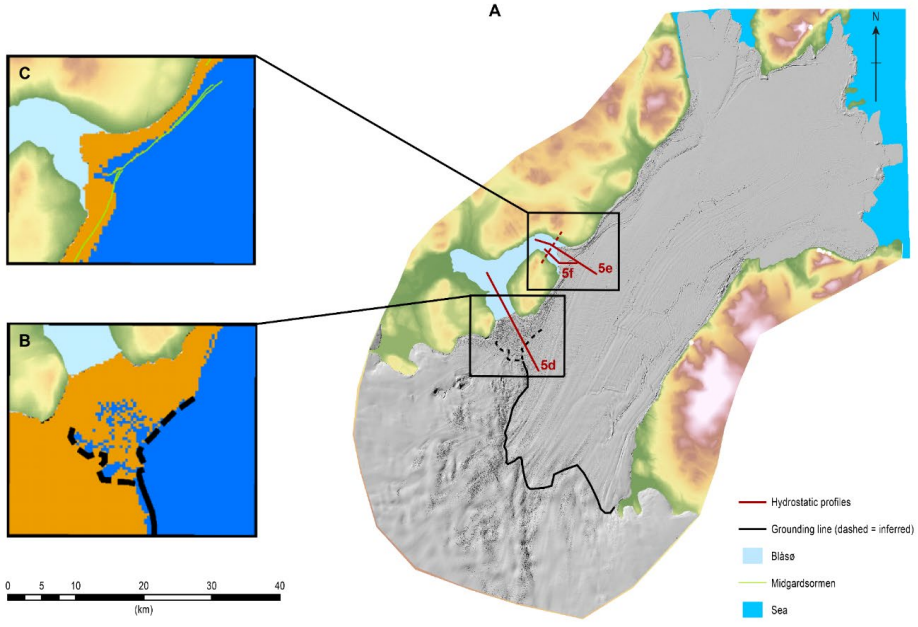

https://doi.org/10.5194/tc-2022-206
Preprint. Discussion started: 1 November 2022

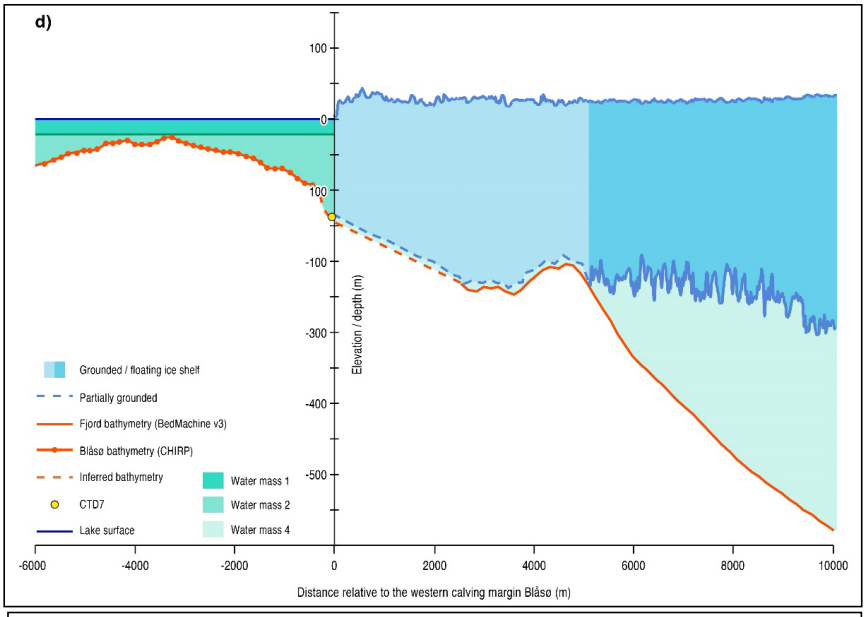

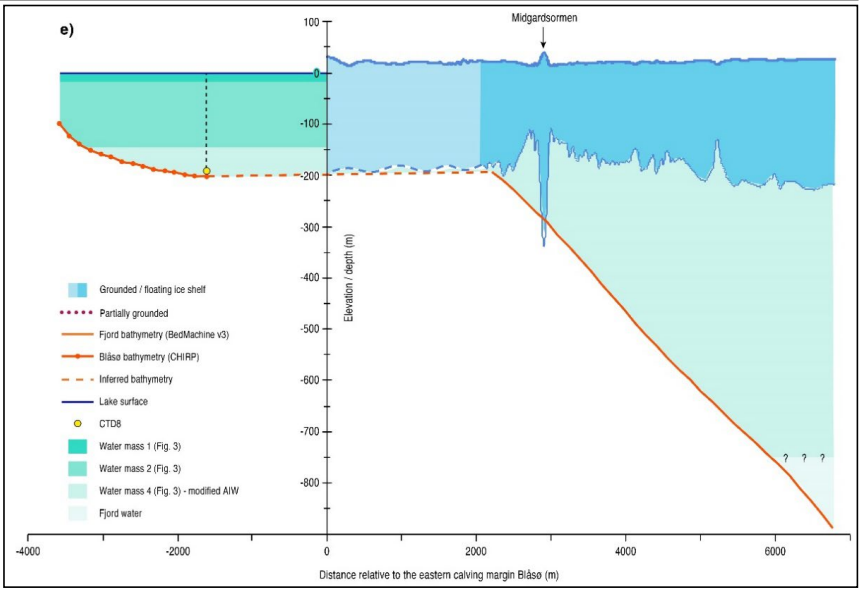

https://doi.org/10.5194/tc-2022-206
Preprint. Discussion started: 1 November 2022

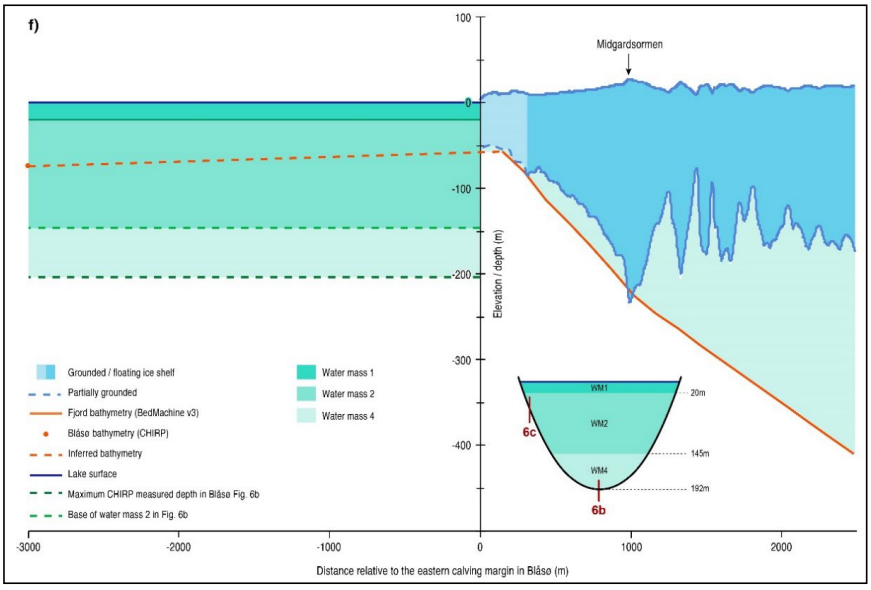

Figure 5. Hydrostatic analysis of the ice shelf calving margins in Blåsø. (**a**) Map showing the ice sheet and ice shelf surface as a grayscale hill shade from Arctic DEM. (**b**) and (**c**) show hydrostatic calculations of grounding for the western and eastern calving fronts in Blåsø, where orange indicates grounded ice and blue indicates floating ice. Note the scale bar applies to a. The western calving margin appears to be more grounded than floating, and the location of the eastern calving margin is close to having a fully floating connection, associated with recent migration of the Midgardsormen (yellow line) towards the northern side of the fjord. Panels (d), (e) and (f) show grounding line relationships in Blåsø, derived from hydrostatic analysis across the locations shown in panel (a). Profiles show the ice shelf surface (from the Arctic DEM), the ice shelf base (calculated from the ice surface elevation assuming hydrostatic equilibrium), and an inferred ice shelf base where the ice is no longer in hydrostatic equilibrium. The bathymetry of the fjord (BedMachine) and the lake (our data, fig 1) are also shown with an inferred bed between the lake and areas where hydrostatic analysis shows floating ice. (**d**) profile across the western margin of Blåsø where the maximum depth for the western basin (136 m) is constrained by CTD7. Despite being grounded for some distance between the lake calving margin and the fjord a temporary or periodic connection must exist to account for the brackish water present in water mass 3 and the dying fish observed in the western basin. (**e**) shows the eastern margin of Blåsø where the grounding line is defined by the Midgardsormen in the Arctic DEM. The halocline in the eastern basin of Blåsø and presence of AIW as water mass 4 implies an open connection between the lake and the sub-shelf cavity must exist. **(f).** Profile across the eastern calving front at the point where the extent of grounded ice is narrowest (see Fig 5). The profile runs along the southern fjord wall of Blåsø and so the ice shelf at the calving front is grounded in only ~50m of water. The profile shows the depths of the deepest part of the eastern basin and the 145m halocline taken from Fig 6b and projected onto this section line.

https://doi.org/10.5194/tc-2022-206
Preprint. Discussion started: 1 November 2022

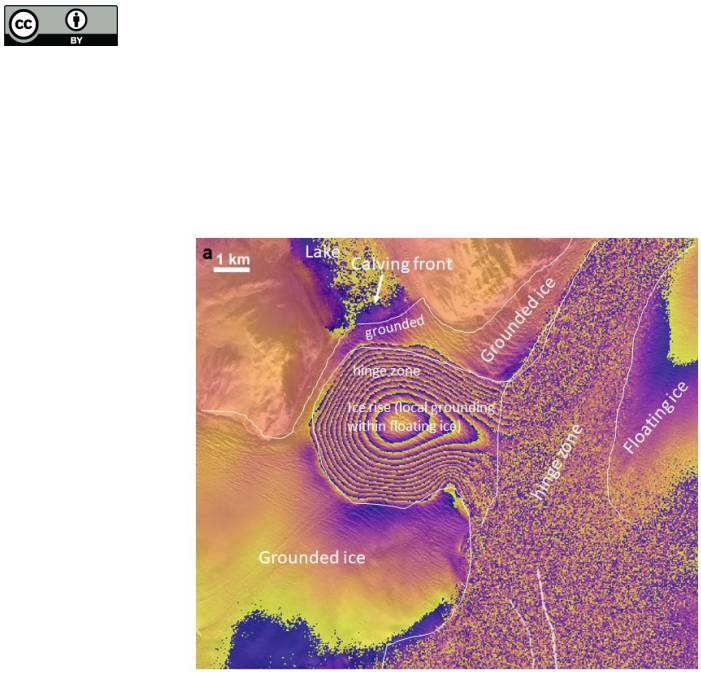

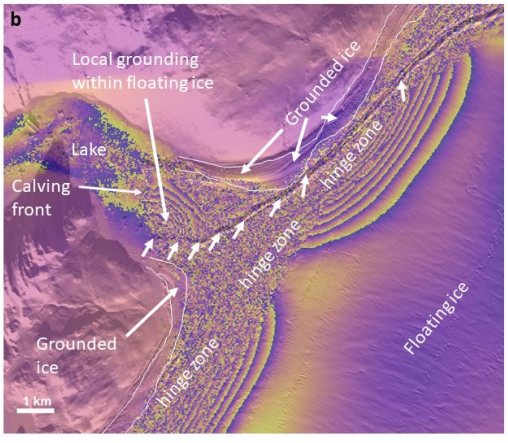

600 **Figure 6**. Interferometric analysis of calving margins in Blåsø. (**a**) Interferogram for western calving margin, and (**b**) Interferogram for eastern calving margin. These show double differential interferograms from Sentinel-1 data collected on 3, 9, and 15 April 2017, superimposed on a Sentinel-2 scene. Annotations show interpreted zones of grounded and floating ice and the hinge zone. In E, short arrows show possible grounding of the Midgardsormen.

605

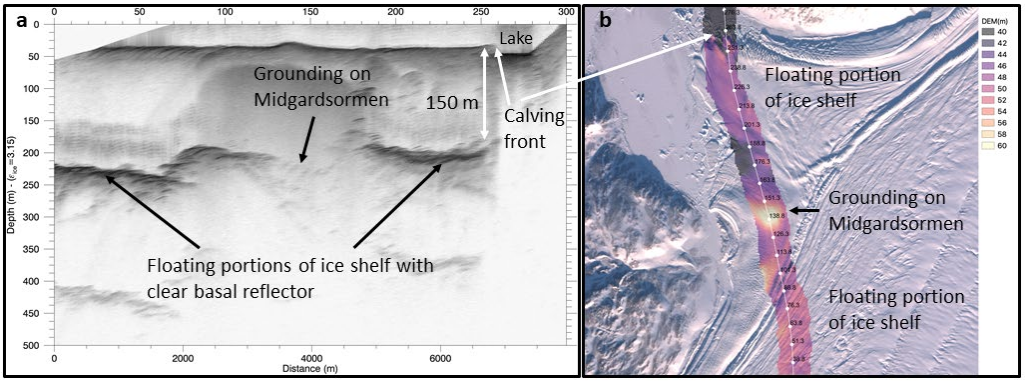

Figure 7. Airborne ice radar over the eastern calving margin in Blåsø. (**a**) Radargram from the AWI UWB multifrequency radar along the flightline shown in panel b. Clear basal reflectors and a zone of grounding (with elevated surface 'bump') are visible. The draught of the ice shelf, assuming a uniform velocity of radio waves in
610 ice is ~150m, closely coincident with the halocline depth measured at sites CTD5 and CTD 8. (**b**) Flight line of radar data, with colour shading of the elevation measured by the laserscanner. The area of grounding identified on interferometry is apparent in the DEM. Data acquired 14th April 2018.

https://doi.org/10.5194/tc-2022-206
Preprint. Discussion started: 1 November 2022

Table 1. CTD locations in Blåsø. All times are UT.

CTD profile ID	Latitude	Longitude	Max depth (m)	Date and time of CTD
CTD1	79 35.738 N	022 35.596 W	15	27/07/2017 15:59
CTD2	79 34.989 N	022 33.173 W	10	31/07/2017 17:42
CTD3	79 32.017 N	022 30.523 W	92	01/08/2017 17:25
CTD4	79 32.067 N	022 32.011 W	126	02/08/2017 16:25
CTD5	79 36.303 N	022 05.251 W	156	07/08/2017 21:35
CTD6	79 31.801 N	022 31.019 W	134	08/08/2017 21:42
CTD7	79 31.774 N	022 30.523 W	136	08/08/2017 22:08
CTD8	79 35.948 N	022 02.767 W	192	10/08/2017 17:26

615